Research Square

Preprints are preliminary reports that have not undergone peer review.
They should not be considered conclusive, used to inform clinical practice,
or referenced by the media as validated information.

Tribological Optimization of FFF-Printed rABS/GR Nanocomposites: Effect of Graphene Loading and Process Parameters via Hybrid GA-ANN

Akash Ahlawat
Maharshi Dayanand University
Ashish Phogat
Maharshi Dayanand University
Upender Punia
Deenbandhu Chhotu Ram University of Science and Technology
Manjeet Chahar
Deenbandhu Chhotu Ram University of Science and Technology
Ravinder Kumar Sahdev
Maharshi Dayanand University
Deepak Chhabra
deepak.chhabra@mdurohtak.ac.in

Maharshi Dayanand University

Research Article

Keywords: Nanocomposite, FFF, Genetic Algorithm, GA-ANN, rABS/GR, Wear Rate

Posted Date: June 2nd, 2026

DOI: https://doi.org/10.21203/rs.3.rs-9394328/v1

License: This work is licensed under a Creative Commons Attribution 4.0 International License.
Read Full License

Additional Declarations: No competing interests reported.

Abstract

This study investigates the tribological behavior of Graphene-reinforced Recycled Acrylonitrile Butadiene Styrene (rABS/GR) nanocomposites fabricated via Fused Filament Fabrication (FFF). The rABS/GR nanocomposite filament was prepared through mechanical blending and melt extrusion using a 3devo filament extruder. Wear test specimens were fabricated using an FFF 3D printer in accordance with ASTM G99 standards, and tribological evaluation was conducted using a DUCOM Pin-on-Disc tester (Model Tr-20LE). The experimental design was established using a Central Composite Design (CCD) matrix in Design-Expert software, examining the effects of Graphene concentration (1–5 wt.%), infill density (40–100%), print speed (20–80 mm/s), and wall count (2–6) on the resulting wear rate. The minimum experimentally recorded wear rate of 0.030 mm^3/m was achieved at 5 wt.% GR concentration, 100% infill density, 30 mm/s print speed, and 6 wall count. An Artificial Neural Network (ANN) model was subsequently trained and validated on the experimental CCD dataset to predict wear performance accurately. A hybrid Genetic Algorithm–ANN (GA-ANN) framework was then developed to optimize the GR concentration and FFF process parameters mathematically. The GA-ANN optimization identified the global minimum wear configuration at 5 wt.% GR concentration, 100% infill density, 20 mm/s print speed, and 5 wall count, yielding a predicted minimum wear rate of 0.0269 mm^3/m. Experimental validation of these optimized parameters produced an actual wear rate of 0.028 mm^3/m, confirming the model's predictive accuracy with an error of approximately 4.09%.

1. Introduction

Additive Manufacturing (AM), particularly Fused Filament Fabrication (FFF), also known as Fused Deposition Modeling (FDM), has rapidly evolved from a prototyping technique into a versatile method for producing functional end-use components across various industries, including automotive, aerospace, and biomedical engineering [1–4]. Acrylonitrile Butadiene Styrene (ABS) is among the most widely utilized thermoplastics in FFF owing to its favourable mechanical strength, dimensional stability, and processability [5–7]. However, growing environmental concerns and regulatory pressure have intensified the drive toward sustainable manufacturing practices. This study employs recycled ABS (rABS) as a matrix polymer, thereby reducing reliance on virgin plastics while maintaining acceptable mechanical characteristics, in line with the circular economy paradigm.

A significant limitation of unreinforced polymer components, including rABS, is their inadequate performance under tribological loading conditions. When subjected to sliding or rolling contact, polymer surfaces undergo progressive material removal, leading to dimensional inaccuracy and eventual component failure [8,9]. To extend the service life and broaden the application envelope of FFF-fabricated parts, it is essential to enhance their surface hardness, thermal stability, and wear resistance. Polymer nanocomposites represent a well-established approach to achieving these improvements [10–12]. Graphene (GR), a two-dimensional sp2-hybridized carbon allotrope, possesses exceptional in-plane tensile strength and superior load-bearing capability [13,14]. When uniformly dispersed in a polymer matrix

such as rABS, graphene nanoplatelets can significantly enhance the composite's stiffness, interfacial bonding, and wear resistance [15,16].

Despite the well-documented potential of graphene-reinforced polymer nanocomposites, the mechanical and tribological performance of FFF-fabricated parts is critically dependent on the interplay of printing process parameters. Variables such as infill density, print speed, and wall count govern the internal microstructure, porosity level, and inter-layer bonding quality, all of which collectively determine the part's resistance to tribological degradation [17,18]. Optimizing these interdependent variables is inherently complex and requires a systematic, computationally intensive methodology.

Conventional statistical approaches, such as Response Surface Methodology (RSM), are effective for modeling smooth, continuous response surfaces but may not capture the highly nonlinear interactions inherent in composite FFF systems [19]. Machine learning-based approaches, particularly Artificial Neural Networks (ANNs), have demonstrated superior capabilities for modeling complex, multivariate relationships [20]. Furthermore, hybrid ANN-metaheuristic frameworks, such as the Genetic Algorithm–ANN (GA-ANN) approach, have been successfully applied to identify globally optimal process parameters that classical gradient-based methods may fail to locate [21].

This research addresses the dual challenge of material enhancement and process optimization. A sustainable rABS/GR nanocomposite filament was developed and characterized. The Central Composite Design (CCD) methodology was employed to systematically study the effects of GR concentration and key FFF parameters on wear rate. A GA-ANN predictive-optimization framework was then applied to identify the parameter set yielding the minimum wear rate. The predicted optimum was subsequently validated through confirmatory physical experiments.

2. Materials and Methods

2.1. Raw Materials

The matrix polymer employed in this study was recycled Acrylonitrile-Butadiene-Styrene (rABS), sourced from pre-production and post-consumer FFF printing waste. This waste stream comprised unfinished or defective parts, support structures, purge lines, brims, and skirts generated during production, as shown in Fig. 1. The collected material, consisting primarily of ABS with minor PLA contamination, was subjected to preliminary cleaning, drying, and mechanical shredding to yield granular feedstock suitable for melt compounding and extrusion. The use of rABS as a matrix aligns with waste-reduction strategies in polymer processing.

The reinforcing agent was high-purity graphene nanopowder (GR), procured from Vedayukt India Private Limited (Jamshedpur, Jharkhand, India). The supplier-specified purity was ≥ 99 wt.%. The graphene was used as-received, without additional surface treatment or chemical functionalization before blending, following the approach adopted in analogous GR-polymer nanocomposite studies [16].

2.2. rABS/GR Nanocomposite Filament Preparation

The rABS/GR nanocomposite was formulated by incorporating GR nanopowder at varying weight-to-weight (w/w) concentrations (1, 3, and 5 wt.%) relative to the rABS matrix. Before blending, the rABS granules were pre-dried at 80°C for 4 hours in a conventional laboratory oven to minimize residual moisture and prevent hydrolytic degradation during extrusion. The dried rABS and the pre-weighed GR nanopowder were then manually blended, as shown in Fig. 2, until visual homogeneity was achieved, with care taken to minimize agglomerate formation.

The blended mixture was subsequently fed into a 3devo Filament Extruder, as shown in Fig. 3, wherein the material was melted, homogenized through the screw-barrel assembly, and extruded into nanocomposite filaments with a nominal diameter of 1.75 mm, suitable for direct use in the FFF printer.

2.3. Filament Characterization

The fabricated nanocomposite filaments were visually and dimensionally inspected to confirm diameter consistency along the filament length. Filament diameter uniformity is critical for consistent material feed rate and deposition quality during FFF printing. The density of each nanocomposite formulation was measured using the Archimedes displacement method, and the resulting values were subsequently used to convert mass loss to volumetric wear loss in the tribological evaluation.

2.4. Specimen Design and Manufacturing

The wear test specimen geometry was designed in accordance with ASTM G99 for pin-on-disc testing using SolidWorks CAD software. The resulting solid model was exported in Standard Tessellation Language (STL) format and imported into Ultimaker Cura slicing software for G-code generation. The rABS/GR nanocomposite filaments were loaded into a Delta Wasp 2040 Industrial X FFF 3D printer, as depicted in Fig. 4. Print parameters were set according to the experimental design matrix, as documented in Table 1, with the nozzle temperature and bed temperature maintained constant at 230°C and 80°C, respectively, for all specimens.

2.5. Tribological Evaluation (Wear Rate Testing)

The tribological behavior of the fabricated rABS/GR nanocomposite specimens was evaluated using a DUCOM Pin-on-Disc tester (Model Tr-20LE), as represented in Fig. 5, in accordance with ASTM G99. Cylindrical pin specimens, with a diameter of 8 mm and a length of 30 mm, were prepared and mounted against a hardened steel disc. The following tribological test parameters were held constant across all experiments: sliding speed of 400 rpm, wear track diameter of 75 mm, normal applied load of 40 N, and test duration of 4 minutes, all conducted under ambient laboratory conditions.

Wear was quantified by measuring the mass of each pin specimen before and after each test using a precision analytical balance. The volumetric wear loss (V) was calculated by dividing the mass loss (Δm)

by the measured density (ρ) of the respective nanocomposite. The wear rate (WR) was subsequently determined using Eq. (1):

$$Wear\ Rate\ =\ \frac{Wear\ Volume\ Loss}{Sliding\ Distance}\ \raisebox{1ex}{mm^3}/\raisebox{-1ex}{m}$$

1

The resulting wear rate values varied with combinations of GR Concentration (%), infill density (%), print speed (mm/s), and wall count. The average wear rate, calculated from triplicate runs for each parameter setting, is systematically reported in Table 1.

2.6. Experimental Design: Central Composite Design (CCD)

A Central Composite Design (CCD) within the Response Surface Methodology (RSM) framework was employed to explore the experimental space systematically. The four input variables were: GR concentration (1–5 wt.%), infill density (40–100%), print speed (20–80 mm/s), and wall count (2–6). The CCD matrix was generated using Design-Expert® software and yielded 30 experimental runs, including factorial points, axial (star) points, and replicated center points for error estimation [19]. The resulting wear rate data are presented in Table 1.

Table 1
Experimental Design Matrix and Wear Rate Results (Actual vs. ANN Predicted)

S. No.	GR Concentration (%)	Infill Density (%)	Print Speed (mm/s)	Wall Count	Wear Rate (mm^3/m)	
					Actual	Predicted by ANN
1.	1	100	30	2	0.048	0.039500009
2.	3	70	55	4	0.042	0.040599991
3.	3	70	55	4	0.042	0.040599991
4.	3	70	80	4	0.049	0.049000021
5.	1	40	80	2	0.081	0.076999993
6.	5	100	20	2	0.031	0.032500009
7.	5	100	30	6	0.030	0.031500004
8.	1	40	30	2	0.065	0.061000017
9.	3	70	55	4	0.042	0.040599991
10.	1	40	80	6	0.075	0.073999986
11.	3	40	55	4	0.058	0.057999876
12.	1	100	20	6	0.038	0.033500004
13.	3	100	55	4	0.032	0.039633998
14.	5	40	80	2	0.077	0.076999993
15.	1	100	80	2	0.045	0.040000024
16.	5	40	30	2	0.061	0.061000017
17.	3	70	55	4	0.042	0.040599991
18.	5	40	30	6	0.059	0.062999994
19.	5	70	55	4	0.035	0.040599991
20.	3	70	55	6	0.040	0.040000057
21.	1	40	20	6	0.063	0.062999994
22.	1	100	80	6	0.041	0.038999972
23.	1	70	55	4	0.047	0.044599991
24.	3	70	55	4	0.042	0.040599991

S. No.	GR Concentration (%)	Infill Density (%)	Print Speed (mm/s)	Wall Count	Wear Rate (mm^3/m)	
					Actual	Predicted by ANN
25.	5	100	80	2	0.035	0.040000024
26.	5	40	80	6	0.074	0.073999986
27.	3	70	30	4	0.035	0.033704693
28.	3	70	55	2	0.045	0.044999967
29.	3	70	55	4	0.042	0.040599991
30.	5	100	80	6	0.031	0.033999972

3. Results

3.1. Effect of Process Parameters on Wear Rate

The 30-run CCD experiment produced wear rates ranging from 0.030 to 0.081 mm^3/m across the investigated parameter space as repoted in Table 1. The minimum experimentally recorded wear rate of 0.030 mm^3/m was observed at the configuration of 5 wt.% GR, 100% infill density, 30 mm/s print speed, and 6 wall count (Run 7). Conversely, the maximum wear rate of 0.081 mm^3/m was recorded at 1 wt.% GR, 40% infill density, 80 mm/s print speed, and 2 wall count (Run 5), representing a 2.7-fold difference across the experimental range.

Infill density emerged as the most dominant parameter. Specimens printed at 40% infill exhibited wear rates of 0.058–0.081 mm^3/m, substantially higher than those at 100% infill (0.030–0.048 mm^3/m). This behavior is attributed to the lower volumetric density and reduced load-bearing cross-section of low-infill structures, which are more susceptible to compressive crushing and subsurface delamination during tribological contact. Print speed also exerted a notable influence: reducing the speed from 80 mm/s to 20 mm/s consistently lowered wear rates by approximately 10%, owing to improved inter-layer fusion and reduced thermal gradient during deposition. Higher GR concentration (5 wt.%) yielded improved wear resistance compared with lower concentrations (1 wt.%), consistent with the well-established role of graphene as a solid lubricant and reinforcing agent in polymer matrices [15].

3.2. ANN Model Development and Training

An ANN was developed using MATLAB® Neural Network Toolbox to model the non-linear relationship between the four FFF/GR process inputs and the wear rate output. The 30-point experimental dataset was partitioned as follows: 70% (21 runs) for training, 15% (4–5 runs) for validation, and 15% (4–5 runs) for independent testing. The final ANN architecture comprised one input layer (4 neurons), two hidden

layers (10 and 6 neurons, respectively), and one output layer (1 neuron). Sigmoid transfer functions (tansig) were employed in the hidden layers, and a linear transfer function (purelin) was used in the output layer. Network training was performed using the Levenberg–Marquardt backpropagation algorithm, with Mean Squared Error (MSE) as the performance criterion. Early stopping was applied using the validation dataset to prevent overfitting.

3.3. ANN Model Validation and Performance

The training state plot, as illustrated in Fig. 6, confirmed successful network convergence, characterized by a monotonic reduction in the MSE performance function and a stable gradient over successive epochs. The error histogram, as represented in Fig. 7, showed that the prediction residuals for all three data partitions were symmetrically distributed around zero, with no systematic bias, confirming the absence of model overfitting.

The performance curves, as shown in Fig. 8, confirmed that the best validation performance was achieved early in training, with no subsequent divergence, indicating a well-generalized model. Regression analysis, as illustrated in Fig. 9, comparing ANN outputs against experimental targets yielded high correlation coefficients ($R > 0.97$) across all three data subsets, confirming the model's superior predictive accuracy and generalization capability for wear rate estimation of rABS/GR nanocomposites fabricated by FFF.

4. Discussion

4.1. Tribological Behaviour and Parameter Effects

The incorporation of graphene nanopowder into the rABS matrix produced a measurable improvement in wear resistance, consistent with reports in the literature on graphene-reinforced polymer composites. The synergistic combination of optimal GR concentration (5 wt.%) with high infill density (100%) and low print speed (20 mm/s) consistently yielded the lowest wear rates in the experimental matrix, demonstrating that material composition and process parameters must be co-optimized to realize the full tribological potential of the nanocomposite.

The dominant role of infill density is physically consistent: higher infill increases the effective load-bearing cross-sectional area. It reduces the internal void fraction, thereby improving compressive strength and resistance to subsurface crack propagation during sliding contact. The beneficial effect of reduced print speed (20 mm/s vs. 80 mm/s) is attributed to longer available time for thermal welding of successive deposited layers, yielding stronger inter-layer adhesion and a more homogeneous microstructure with fewer stress-concentration sites.

4.2 GA-ANN Optimization

The validated ANN model was integrated as a fitness function evaluator within a Genetic Algorithm (GA) optimization framework to identify the globally optimal process parameter combination minimizing wear

rate. The GA was configured with a population size of 50 individuals, a maximum of 100 generations, a crossover probability of 0.85, and a mutation probability of 0.01, with the parameter bounds constrained to the experimental ranges. The optimization successfully converged after 92 generations, as illustrated by the fitness convergence plot in Fig. 10. The GA identified the optimal configuration as: 5 wt.% GR concentration, 100% infill density, 20 mm/s print speed, and 5 wall count, with a predicted minimum wear rate of 0.0269 mm^3/m.

It is noteworthy that the GA-identified optimum wall count (5) differs slightly from the experimentally observed minimum (wall count = 6, Run 7). This is consistent with the expected behavior of a GA operating over a continuous parameter space: the GA explores combinations not explicitly represented in the discrete CCD matrix, and can identify solutions in the intermediate parameter space that yield marginally lower predicted wear rates. The convergence to wall count = 5 rather than 6 suggests a non-monotonic local response surface in this region, where the ANN predicts a slight improvement at the intermediate value.

4.3. Experimental Validation

Three confirmatory specimens were fabricated at the GA-ANN optimal settings (5 wt.% GR, 100% infill, 20 mm/s, wall count = 5) and subjected to Pin-on-Disc testing under identical conditions. The experimentally measured mean wear rate was 0.028 mm^3/m, compared with the GA-ANN-predicted value of 0.0269 mm^3/m as documented in Table 2. The corresponding predictive error of 4.09% confirms the strong agreement between the model prediction and the physical experimental outcome, validating the GA-ANN hybrid framework as an effective optimization tool for FFF process parameter selection.

Table 2
Experimental Validation of the GA-ANN Model

Mechanical Testing	Model Prediction	Experimental Result	Error (%)
Wear Rate (mm^3/m)	0.0269	0.028	4.09

5. Conclusion

This study successfully demonstrated the development of a sustainable rABS/GR nanocomposite filament and the establishment of an optimized FFF process to maximize its tribological performance. The incorporation of graphene nanopowder at 5 wt.% into the recycled ABS matrix yielded the most significant improvement in wear resistance within the studied concentration range, confirming the efficacy of graphene as a reinforcing and solid-lubricant filler in rABS-based FFF nanocomposites. Infill density was identified as the most influential FFF process variable governing wear rate. Specimens printed at 100% infill exhibited wear rates up to 2.7 times lower than those at 40% infill, attributable to the higher load-bearing cross-section and reduced subsurface void fraction at full density. The developed two-hidden-layer ANN model demonstrated high predictive accuracy ($R > 0.97$ across training, validation,

and testing partitions), confirming its suitability for surrogate modeling of the complex, non-linear FFF tribological response surface. The hybrid GA-ANN framework successfully identified the globally optimal FFF configuration (5 wt.% GR, 100% infill density, 20 mm/s print speed, wall count = 5), yielding a predicted minimum wear rate of 0.0269 mm^3/m. Experimental validation at this configuration yielded a wear rate of 0.028 mm^3/m, corresponding to a predictive error of only 4.09%, demonstrating the practical reliability of the optimization framework.

The successful utilization of rABS from post-consumer 3D printing waste as a viable matrix polymer demonstrates a practical pathway toward closed-loop material reuse in polymer additive manufacturing, contributing to circular economy objectives without significant sacrifice in mechanical performance. The findings collectively establish that rABS/GR nanocomposites fabricated via FFF can serve as high-performance, sustainable alternatives for components operating under moderate tribological conditions. Future work should investigate multi-response optimization encompassing tensile and flexural properties alongside wear rate, explore alternative eco-friendly reinforcement fillers, and assess the long-term tribological durability of rABS/GR components under varied loading and environmental conditions.

Declarations

Author Contribution

A.A.: Methodology, Investigation, Formal analysis, Writing – original draft, Software, Visualization. A. P.: Methodology, Investigation. U.P.: Methodology, Investigation, Writing – original draft, Resources. M.C.: Data Curation. R.K.S.: Validation, Supervision. D.C.: Writing – review & editing, Investigation, Funding Acquisition, Supervision.

Acknowledgement

The authors acknowledge the Maharshi Dayanand University (including ACIL), Rohtak and Deenbandhu Chhotu Ram University of Science and Technology, Sonipat, for providing essential infrastructure and research facilities.

Data Availability Statement

The data that support the findings of this study are available from the corresponding author upon reasonable request.

References

1. Punia U, Dhull S, Habeeb A et al (2025) Adopting additive manufacturing: Spotlight on sustainability and material utilization. Green Mater ; 1–11

2. Ahlawat A, Phogat A, Narang R et al (2025) Enhancing tensile-tensile fatigue performance of FDM-fabricated carbon fiber-nylon composites using GA-ANFIS optimization. J Mech Sci Technol 39:5143–5150
3. Ahlawat A, Phogat A, Punia U et al Innovative Optimization of Mechanical Performance in Carbon Fiber-Reinforced Nylon Composite Using Artificial Neural Networks and Multi-Objective Genetic Algorithms. J Mater Eng Perform. Epub ahead of print 2025. 10.1007/s11665-025-10973-5
4. Venkateswar Reddy M, Hemasunder B, Mahadevapa Chavan P et al Study on the significance of process parameters in improvising the tensile strength of FDM printed carbon fibre reinforced PLA. *Mater Today Proc*. Epub ahead of print 2023. 10.1016/j.matpr.2023.06.330
5. Ahlawat A, Phogat A, Yadav M et al (2023) Fabrication and analysis of ABS-HDPE-PC composite polymer filament used for FDM printing using hybrid algorithm. Int J Interact Des Manuf 17:3199–3209
6. Narang R, Ahlawat A, Dhingra AK et al Optimization of Process Parameters to Investigate the Fatigue Behavior of Fused Deposition Modeling-Fabricated ABS Parts Using Hybrid Tool. J Mater Eng Perform. Epub ahead of print 2025. 10.1007/s11665-025-10992-2
7. Lobov E, Vindokurov I, Tashkinov M (2024) Mechanical Properties and Performance of 3D-Printed Acrylonitrile Butadiene Styrene Reinforced with Carbon, Glass and Basalt Short Fibers. Polym (Basel) 16:1106
8. Phogat A, Chhabra D, Sindhu V et al (2022) Analysis of wear assessment of FDM printed specimens with PLA, multi-material and ABS via hybrid algorithms. Mater Today Proc 62:37–43
9. Siddiqui MAS, Hossain MAM, Ferdous R et al An extensive review on bibliometric analysis of carbon nanostructure reinforced composites. 25
10. Ahlawat A, Sahdev RK, Gupta RK et al (2021) 3D FDM Printable Polymer Composites and Polymer Nanocomposites: State of the Art. J Nano- Electron Phys 13:1–4
11. Punia U, Garg RK, Phogat A et al (2024) Analyzing the Effect of Addition of Ss 316L Nanoparticles on the Hardness and Impact Strength of 3D Printable Pmma Resin. *Proceedings on Engineering Sciences* ; 6: 1611–1620
12. Siripongpreda T, Hoven VP, Narupai B et al Emerging 3D printing based on polymers and nanomaterial additives: Enhancement of properties and potential applications. Eur Polym J ; 184. Epub ahead of print 2023. 10.1016/j.eurpolymj.2022.111806
13. Ahlawat A, Phogat A, Punia U et al Investigation of mechanical and morphological properties of 3D-printed GR-PLA nanocomposites with process parameter optimization using MOGA-ANN. *Progress in Additive Manufacturing*. Epub ahead of print 2025. 10.1007/s40964-025-01322-y
14. Sudheer Reddy J, Praveena BA, Kedambadi Vasu V et al Mechanical Characterization of Graphene Reinforced PLA Composites Printed by Fused Deposition Modelling. *MysuruCon* (2022) *–2022 IEEE 2nd Mysore Sub Section International Conference*. Epub ahead of print 2022. 10.1109/MysuruCon55714.2022.9972518

15. Harussani MM, Sapuan SM, Nadeem G et al (2022) Recent applications of carbon-based composites in defence industry: A review. Def Technol 18:1281–1300
16. Gutiérrez-Mora F, Morales-Rodríguez A, Gallardo-López A et al (2019) Tribological behavior of graphene nanoplatelet reinforced 3YTZP composites. J Eur Ceram Soc 39:1381–1388
17. Pszczółkowski B, Zaborowska M Effect of Layer Exposure Time in SLA-LCD Printing on Surface Topography, Hardness and Chemical Structure of UV-Cured Photopolymer. *Lubricants*; 13. Epub ahead of print 2025. 10.3390/lubricants13090406
18. Sood AK, Ohdar RK, Mahapatra SS (2010) Parametric appraisal of mechanical property of fused deposition modelling processed parts. Mater Des 31:287–295
19. Khuri AI, Mukhopadhyay S (2010) Response surface methodology. Wiley Interdiscip Rev Comput Stat 2:128–149
20. Alhaddad W, He M, Halabi Y et al (2022) Optimizing the material and printing parameters of the additively manufactured fiber-reinforced polymer composites using an artificial neural network model and artificial bee colony algorithm. Structures. Elsevier, pp 1781–1795
21. Kumar P, Gupta P, Singh I (2023) Performance Analysis of Acrylonitrile–Butadiene–Styrene–Polycarbonate Polymer Blend Filament for Fused Deposition Modeling Printing Using Hybrid Artificial Intelligence Algorithms. J Mater Eng Perform 32:1924–1937

Figures

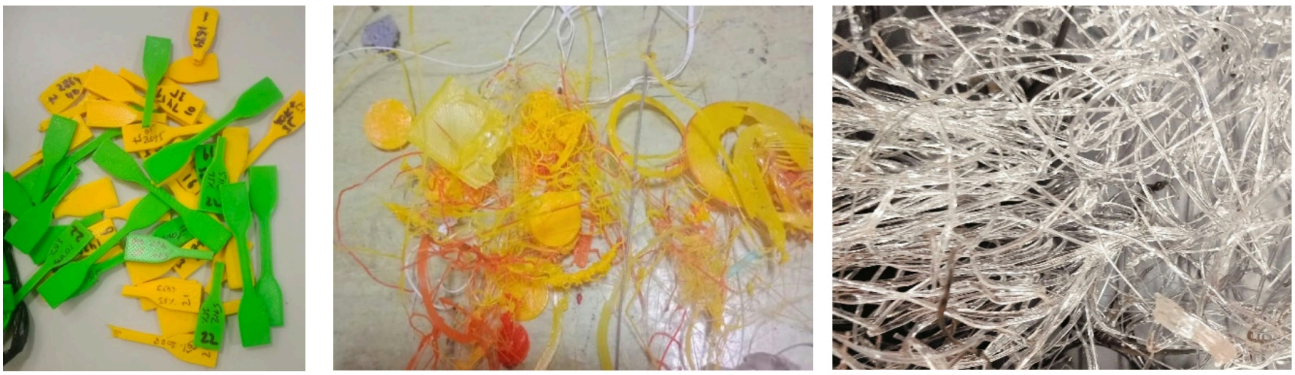


Figure 1

Polymer waste

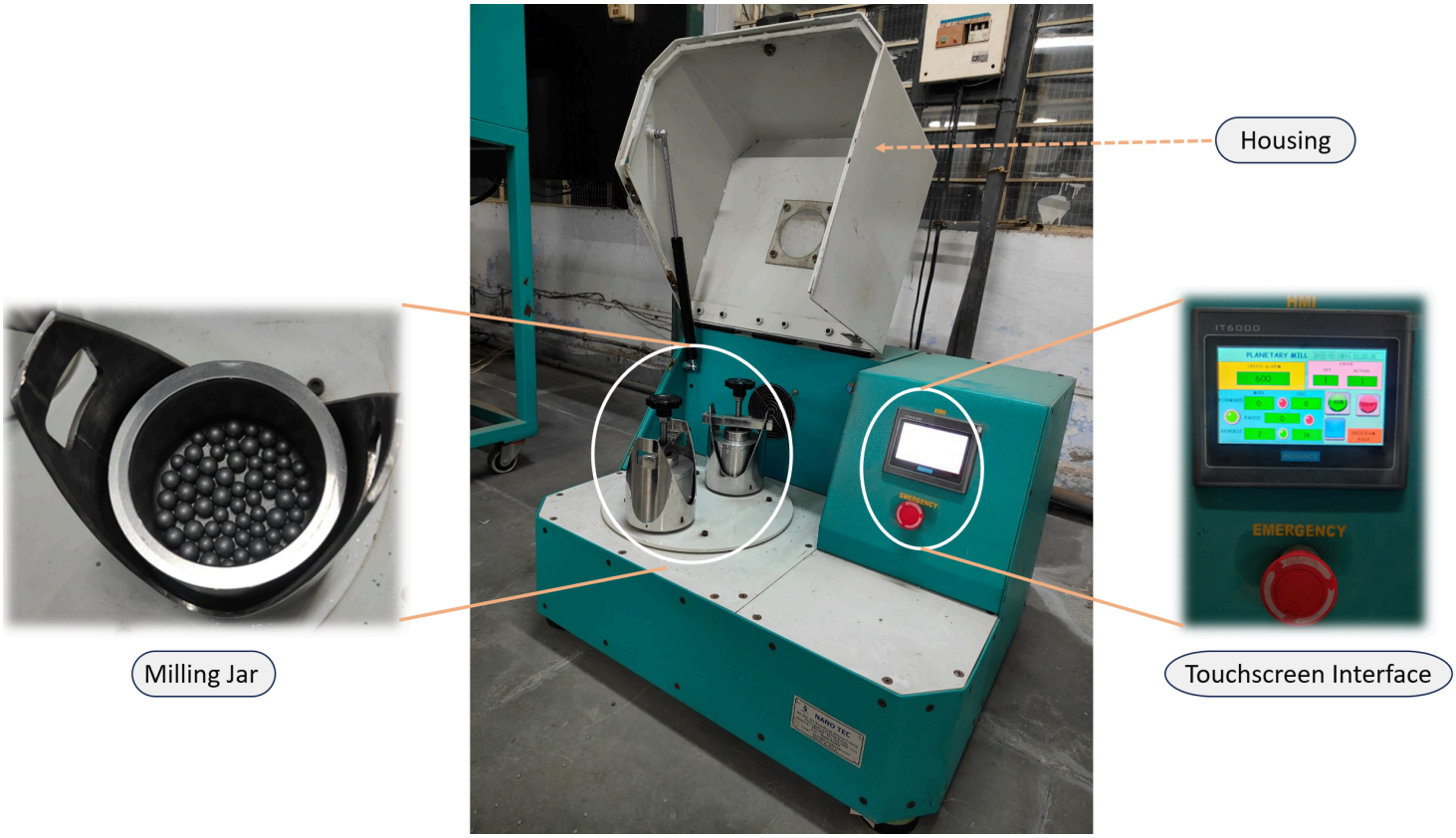


Figure 2

High-Energy Planetary Ball Mill

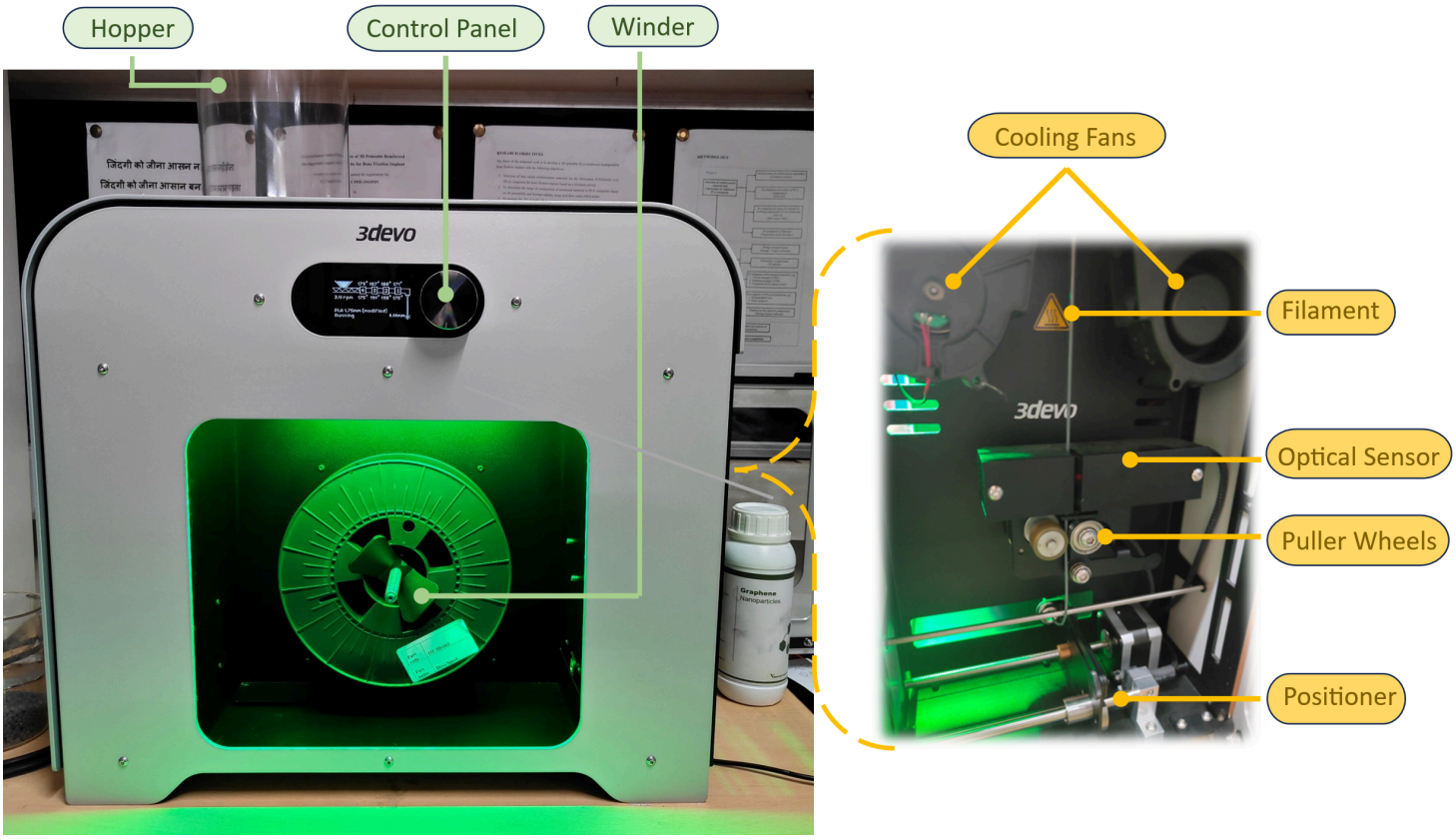


Figure 3

3devo Filament Extruder used for filament fabrication

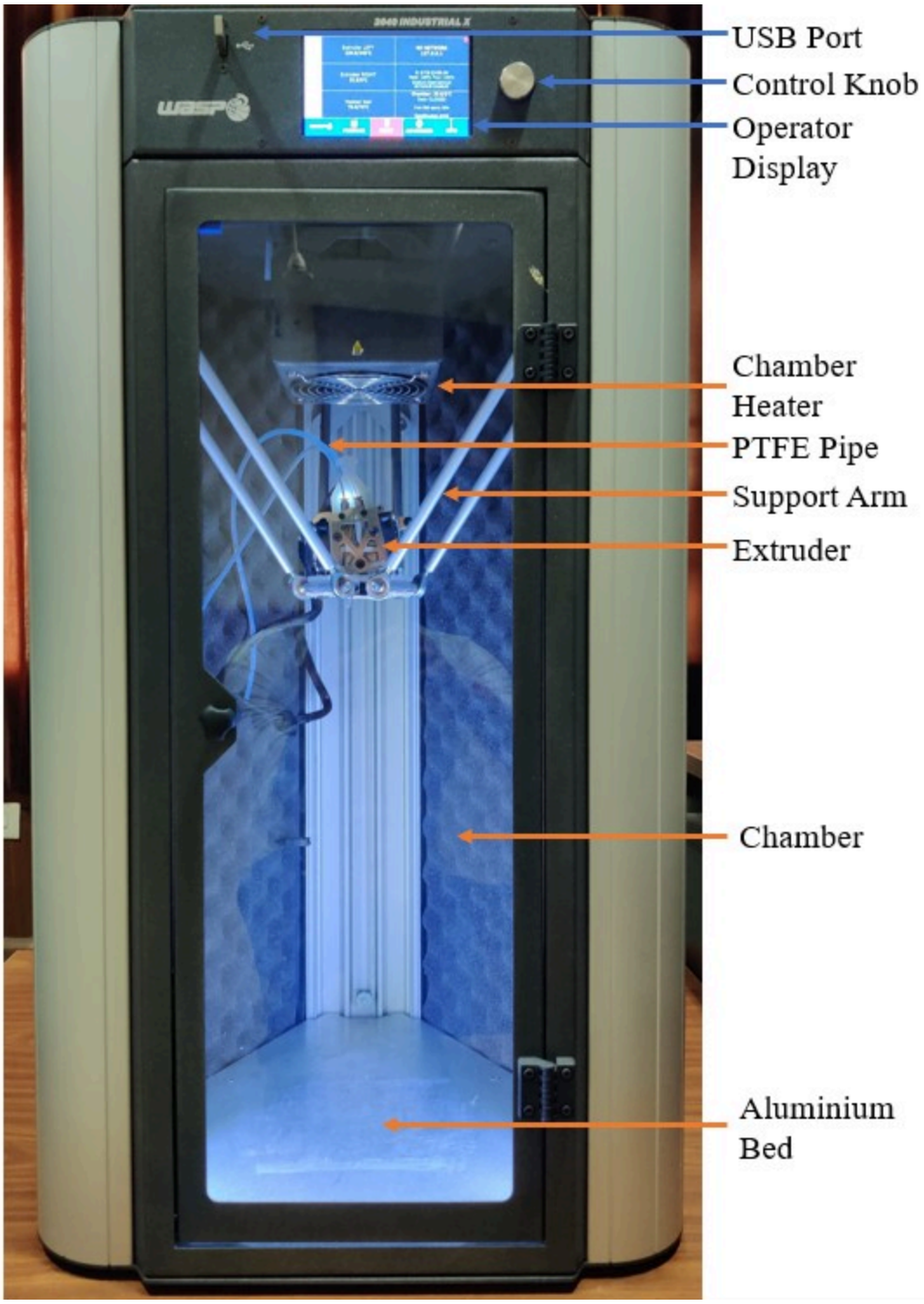


Figure 4

Delta Wasp-2040 industrial X 3D printer used for specimen fabrication

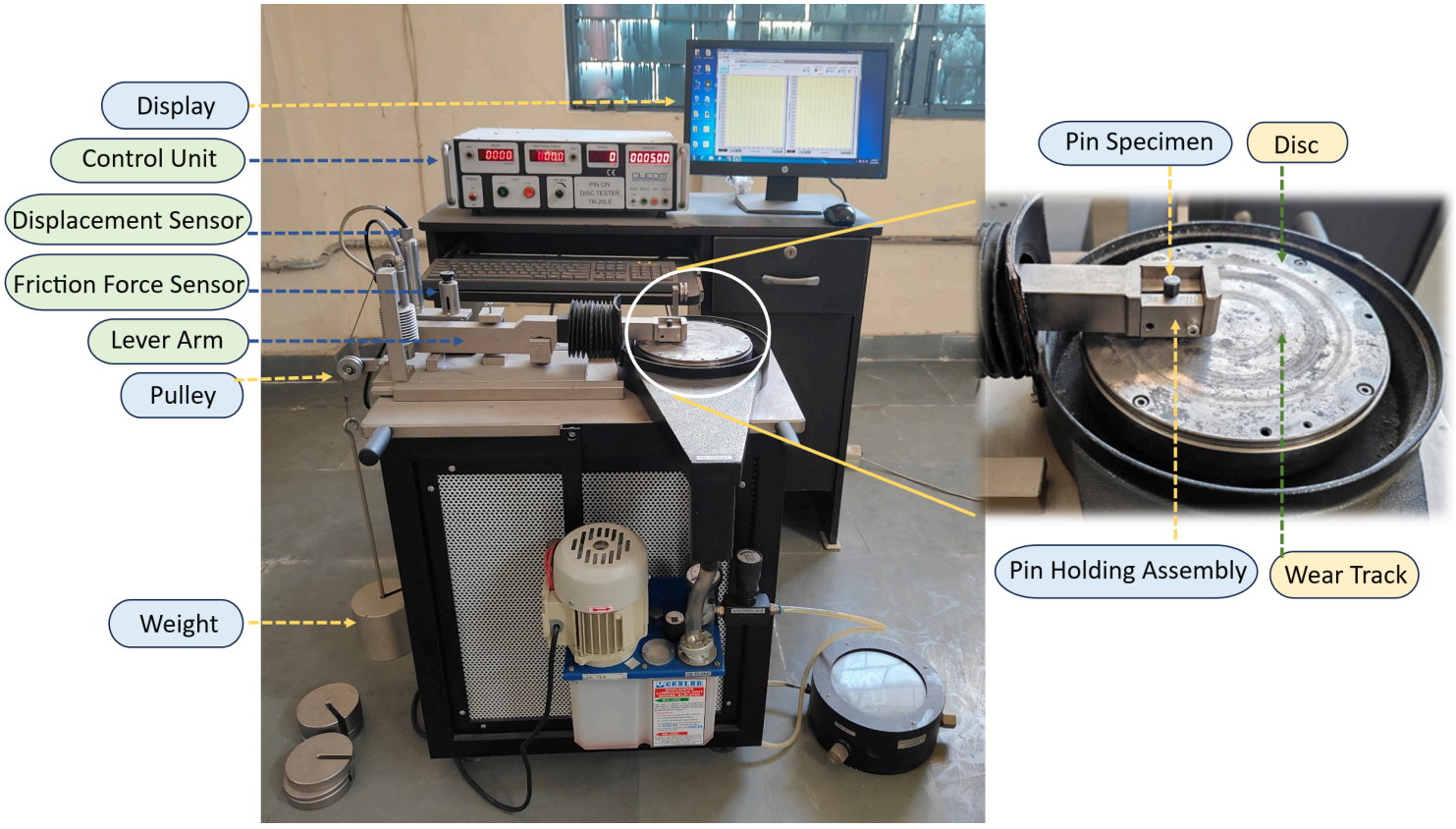


Figure 5

Pin-on-Disc Wear Testing Machine

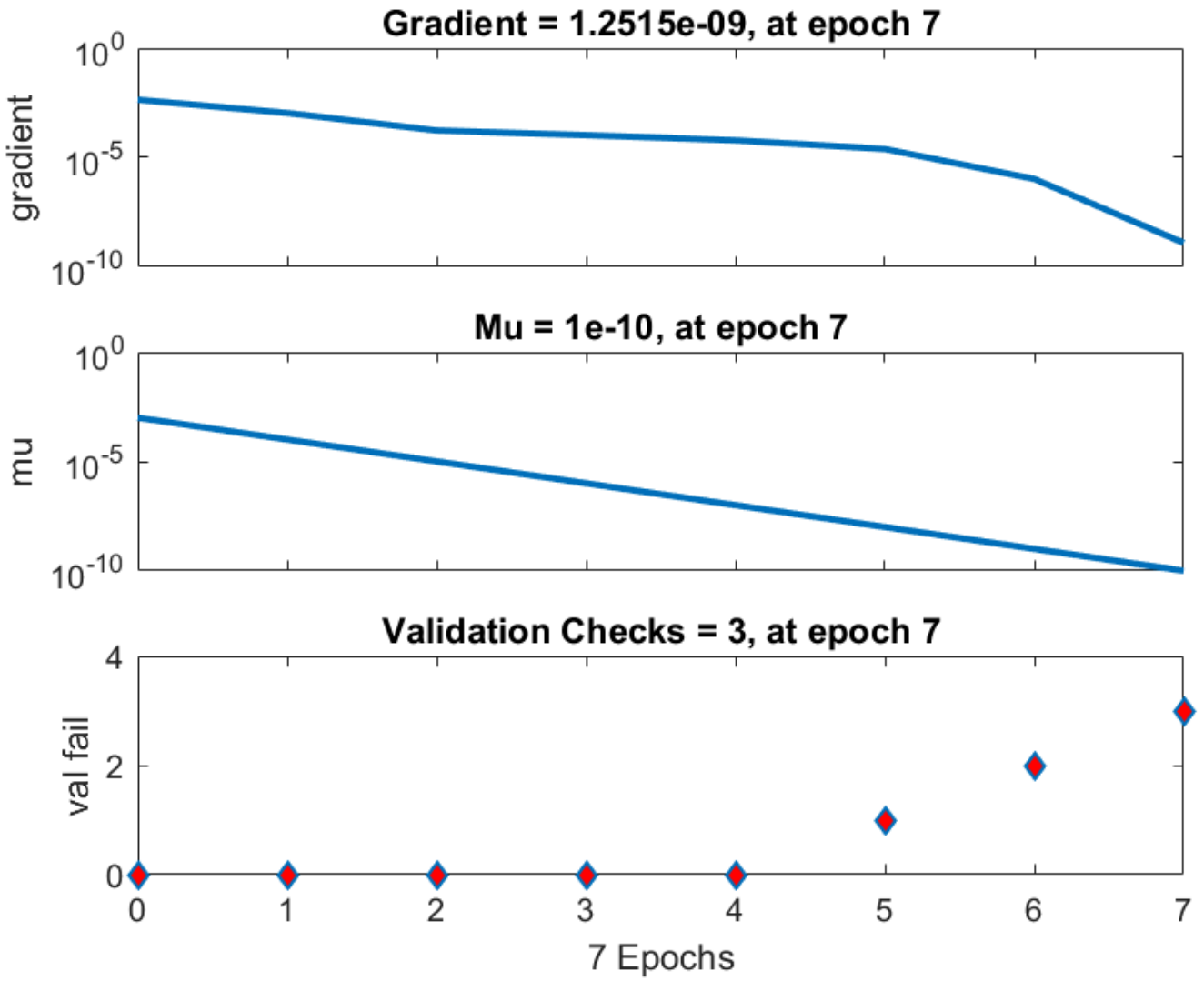


Figure 6

ANN Training state plot showing convergence and gradient stability

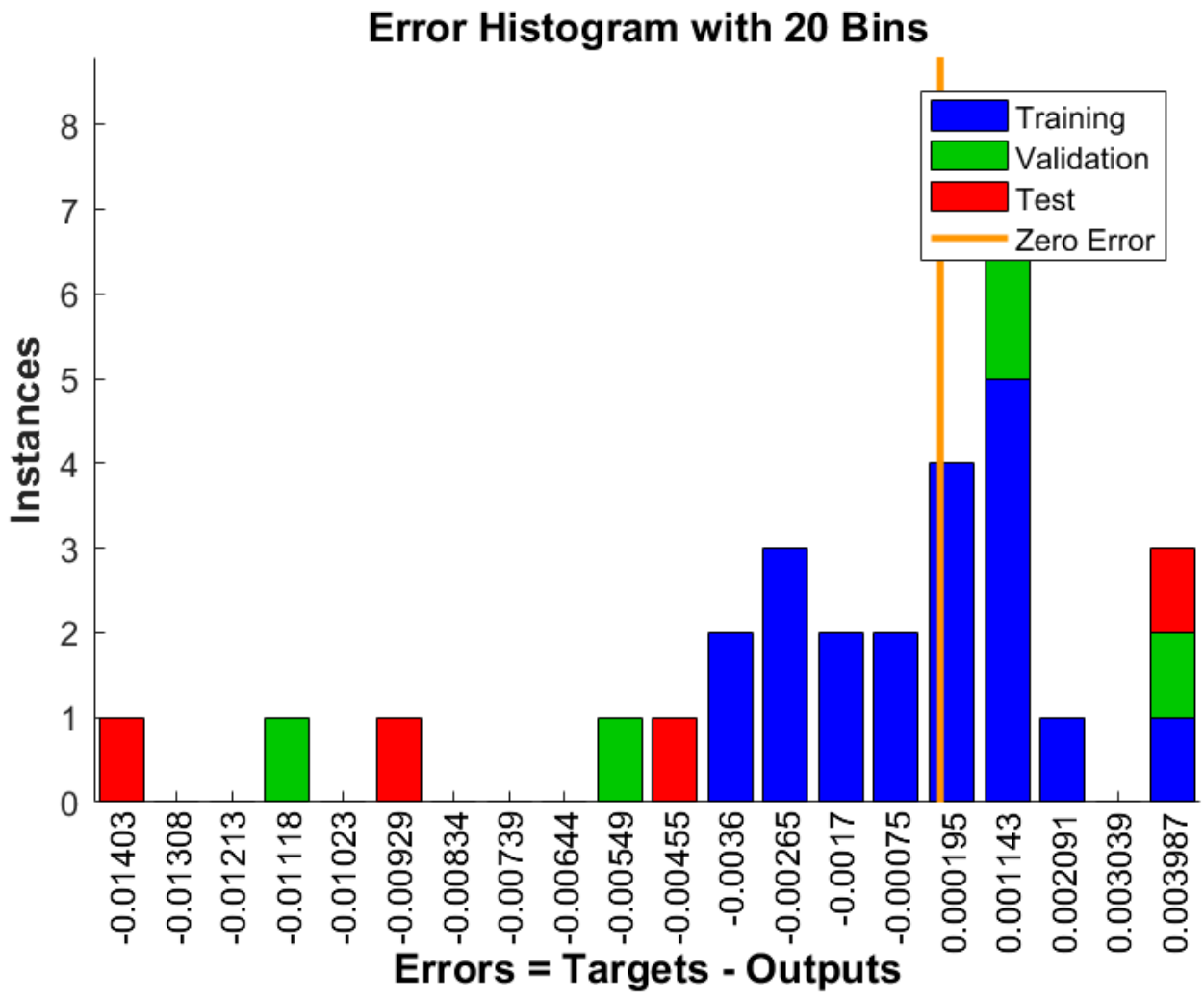


Figure 7

Error Histogram showing distribution of prediction residuals across training, validation, and testing datasets

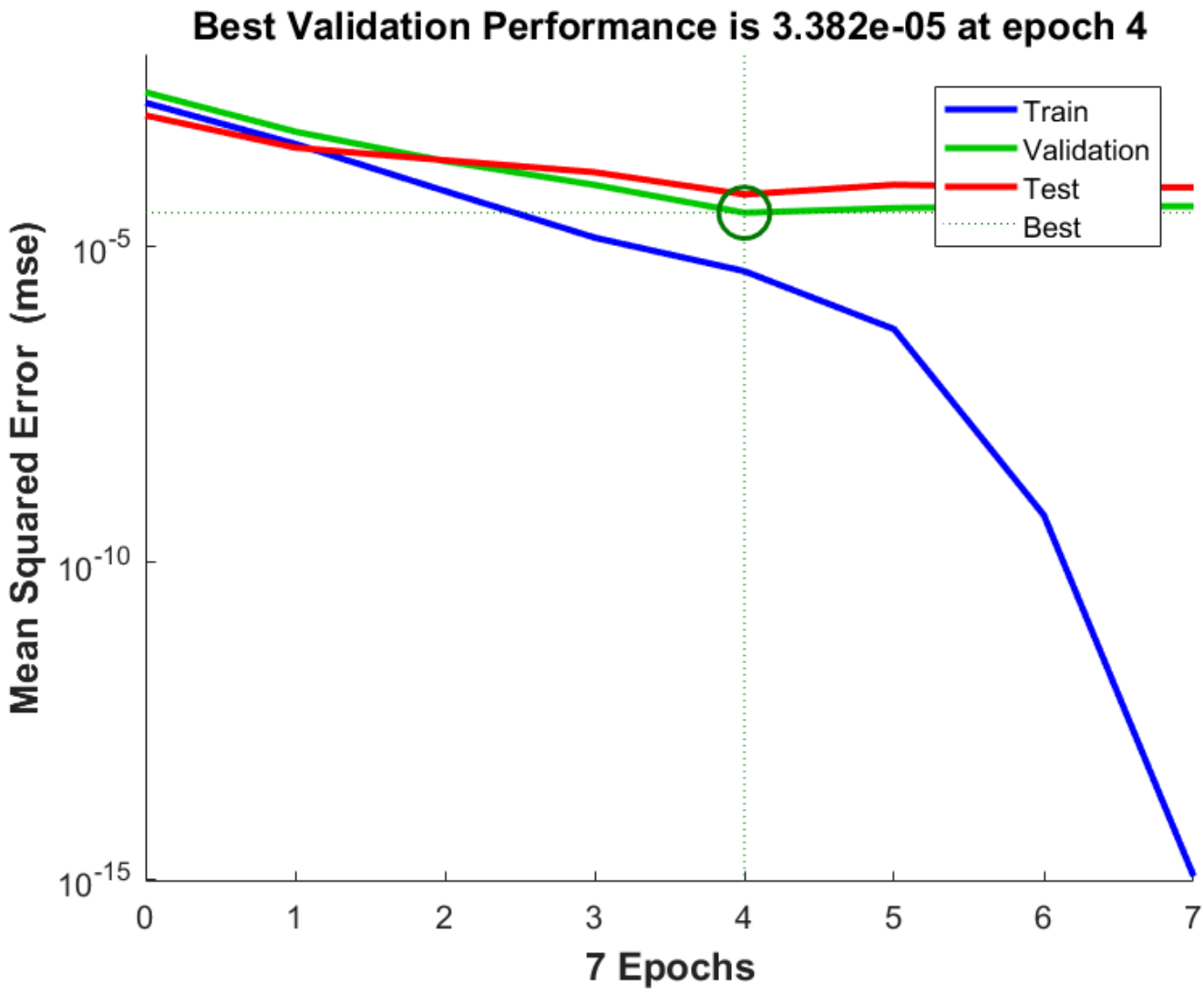


Figure 8

Performance Curves showing MSE progression for training, validation, and testing datasets

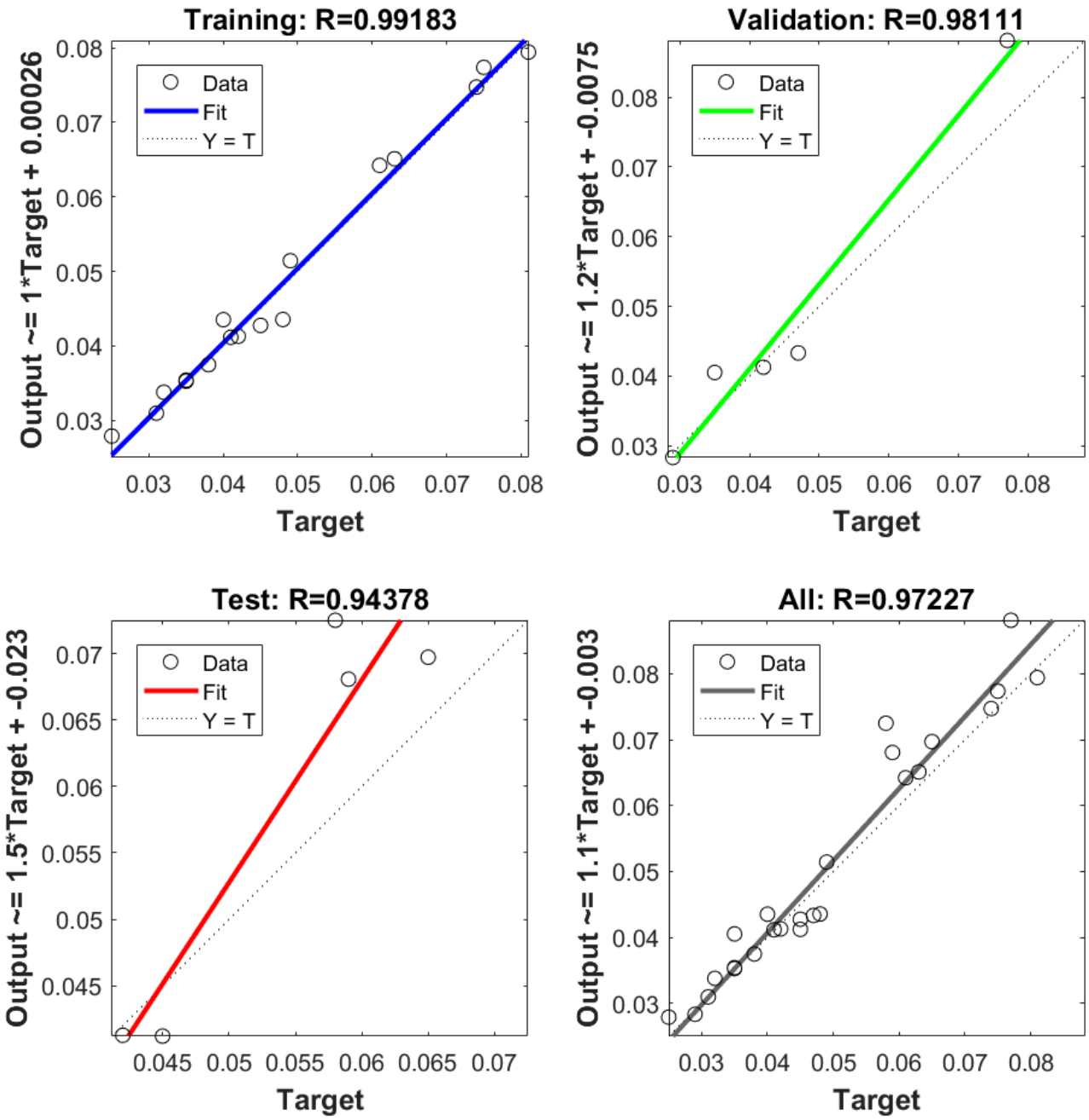


Figure 9

Regression Coefficient plots for training, validation, testing, and overall datasets

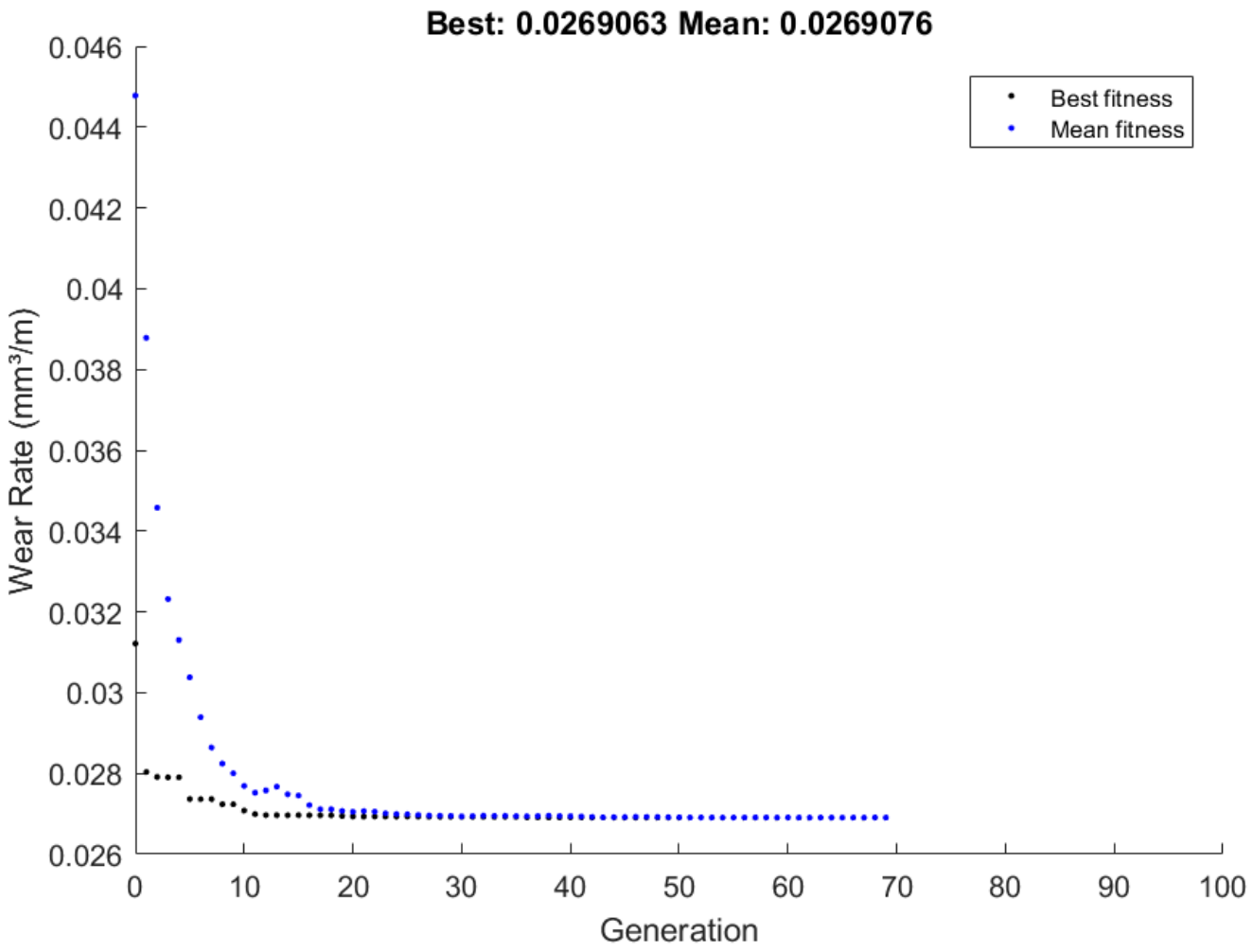


Figure 10

GA-ANN Best Fitness Plot showing convergence of minimum predicted wear rate